

# Lithospheric thickness of the Chinese continent

Meijian An <sup>a,b,\*</sup>, Yaolin Shi <sup>a</sup>

<sup>a</sup> *Laboratory of Computational Geodynamics, Graduate University of Chinese Academy of Sciences, Yuquan Road 19a, Beijing, China*

<sup>b</sup> *Key Laboratory of Crust Deformation and Processes and Institute of Geomechanics, Chinese Academy of Geological Sciences, MinZuDaXue NanLu 11, Beijing 100081, China*

Received 10 June 2006; received in revised form 30 July 2006; accepted 10 August 2006

## Abstract

We invert for the upper-mantle temperatures of the Chinese continent in the depth range of 70–240 km from a recent S-velocity model. The depth where temperatures intersect a mantle adiabat with a potential temperature of  $\sim 1300^\circ\text{C}$  is in close correspondence with the top of the seismic low velocity zone for most regions. This correspondence implies that seismic lithosphere estimated from short-time scale seismic information may be equivalent to the long-time scale geodynamical lithosphere. Defining the  $1300^\circ\text{C}$  adiabat as coinciding with the lithospheric base, we estimate the seismic-thermal lithosphere thickness. The estimated thickness shows obvious dependence on the tectonic settings. Beneath eastern China, which mainly belongs to the circum-Pacific tectonic domain, it has a thickness of  $\sim 100$  km; and beneath the Qinghai–Tibet plateau and south to the Tarim craton, which belong to the Tethyan tectonic domain it has a thickness of  $\sim 160$ – $220$  km. The lithospheric thicknesses of the three large para-platforms/cratons range from  $\sim 170$  km for the western Yangtze,  $\sim 140$  km for Tarim, and  $\sim 100$  km for Sino-Korean. The three cratons may have been reshaped by Phanerozoic tectonic activities and are thinner than most cratons in other continents.

© 2006 Elsevier B.V. All rights reserved.

**Keywords:** Lithospheric thickness; Chinese continent; Temperature; S-velocity

## 1. Introduction

The Chinese continent contains three Precambrian para-platforms/cratons (Yangtze, Tarim, and Sino-Korean) and three Phanerozoic tectonic domains: the Tethyan (active since  $\sim 250$  Ma), Paleo-Asian (active until  $\sim 260$  Ma), and circum-Pacific (active since  $\sim 250$  Ma) (Ren et al., 1999) (Fig. 1). The contemporary tectonic framework and the geographic relief of the Chinese continent are shaped in the Cenozoic by the

subduction of the Pacific and Philippines oceanic plates in the east and the collision with the Indian plate in the southwest. An improved knowledge of the thicknesses and structures of the Chinese lithosphere is very important for a better understanding of the Chinese continental geodynamics. But much confusion has been caused by the different estimates based on different definitions of the lithosphere.

In plate tectonics the lithosphere is defined as the cold and rigid outer shell of the Earth, and remains coherent during geologic activities. One manifestation of the lithospheric rigidity is the flexural response of the earth's surface when it is subjected to vertical loads. By comparing the flexure observed in the vicinity of the loads with the predictions based on simple plate models, the effective elastic lithosphere thickness,  $T_e$ , can be determined

\* Corresponding author at: Institute of Geomechanics, Chinese Academy of Geological Sciences, MinZuDaXue NanLu 11, Beijing 100081, China. Tel.: +86 10 88256475; fax: +86 10 88256012.

E-mail addresses: [meijianan@yahoo.com.cn](mailto:meijianan@yahoo.com.cn) (M. An), [shiyl@gucas.ac.cn](mailto:shiyl@gucas.ac.cn) (Y. Shi).

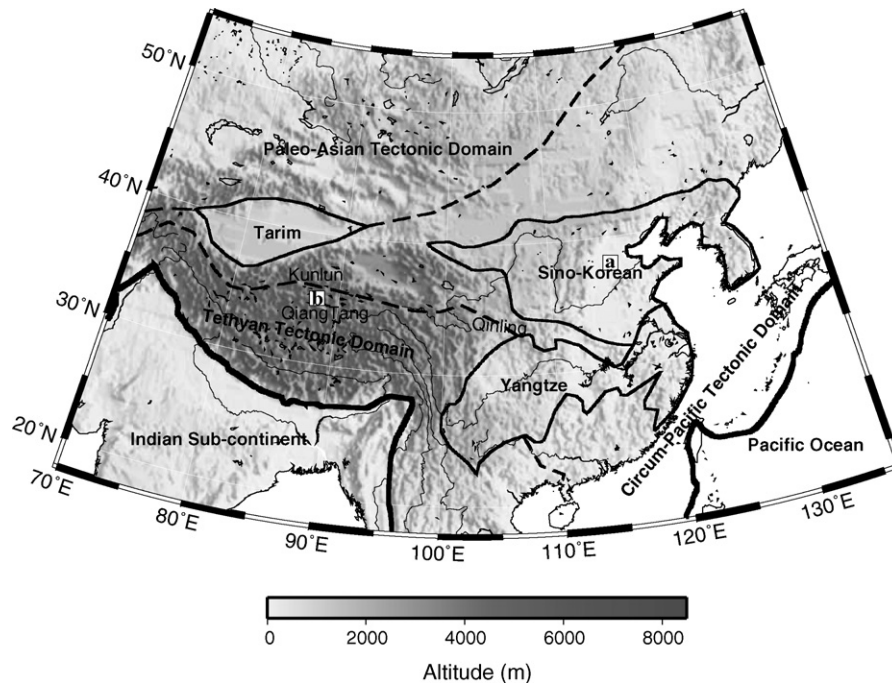


Fig. 1. Map of the topography and tectonic setting in the Chinese continent. The tectonic setting is simplified from Ren et al. (1999). Thick lines are tectonic plate boundaries. Labeled squares are the positions of 1D profiles in Fig. 2.

(Watts and Burov, 2003). The effective elastic lithosphere thicknesses of the Chinese continent have been studied by a number of investigators (Lyon-Caen and Molnar, 1983, 1984; McNutt et al., 1988; Jin et al., 1996; Wang and Xu, 1996; Wang et al., 2001; Braitenberg et al., 2003; Zhao et al., 2004) (Table 1). It varies from as low as 10 km in Tibet to 110 km in the Yangtze craton. Although the estimates of  $T_e$  for the oceanic lithosphere approximately follow the depth to a specific isotherm, which marks the base of the mechanical lithosphere, the physical meaning and the significance of the effective elastic lithosphere for the continents is much more complicated.  $T_e$  in some continental regions may not correspond to any specific structure of the lithosphere but is strongly influenced by the thermal resetting, tectonics, crustal compositions, and the coupling/decoupling of the crust and upper mantle (Burov and Diament, 1995).

In geodynamics, the thermal boundary layer of a convecting mantle is often referred to as the thermal lithosphere and can support large stresses over a long period of time. The lithospheric thermal structure is usually calculated by solving the steady state thermal conduction equation constrained by appropriate boundary conditions (e.g., heat-flow). An adiabatic temperature of mantle potential temperature of  $\sim 1300^\circ\text{C}$  is usually taken to coincide with the base of the thermal lithosphere (Jaupart and Mareschal, 1999; Artemieva and Mooney, 2001). Mareschal and Jaupart (2004) noted that the conductive calculation is valid only in stable continents with ages greater than  $\sim 500$  Ma. For the Chinese continent, most regions are too young to satisfy this condition; even the Yangtze and Tarim cratons may have been reshaped by Phanerozoic tectonic activities (Ren et al., 1999) and then should have a small tectonother-

Table 1  
Lithospheric thicknesses of some geological provinces in China estimated with different definitions

Region	$T_e$	$T_t$	$T_s$
Tibet median massifs	10–30 <sup>(1,2)</sup> , 85 <sup>(3)</sup>	130–175 <sup>(5,6)</sup>	162 <sup>(8)</sup>
Tarim craton	40–50 <sup>(2,3)</sup> , 110 <sup>(1)</sup> , 73 <sup>(4)</sup>	264 <sup>(4)</sup> , 250 <sup>(7)</sup>	190 <sup>(8)</sup>
Sino-Korean craton (north China)	14 <sup>(4)</sup> , 25 <sup>(3)</sup>	110–150 <sup>(5,6)</sup> , 71 <sup>(4)</sup>	80 <sup>(9)</sup>
Yangtze craton	105 <sup>(4)</sup>	110–200 <sup>(5,6)</sup>	90–160 <sup>(8)</sup>

Note: Superscript numbers in parentheses indicate references as follows: (1) Braitenberg et al. (2003); (2) Zhao et al. (2004); (3) Wang and Xu (1996); (4) Wang et al. (2001); (5) Artemieva and Mooney (2001); (6) Wang (1996); (7) Wang (2001); (8) Zhu et al. (2002); (9) Teng (1994);  $T_e$  is the effective elastic thickness,  $T_t$  the thermal lithosphere thickness, and  $T_s$  is the thickness of the seismic lithosphere.

mal age. Furthermore, recent/ancient environment, local geology and topography may change the thermal parameters (e.g., surface heat flow, heat production, conductivity) causing additional errors and uncertainties in the calculated temperatures in upper mantle. A change of 5% in surface heat flow, for example, can cause 50–90 °C variation in the estimated temperature at a depth of 100 km and 10–25 km variation in the estimated lithospheric thickness; a 20% change in the average crustal heat production can cause changes of 100–130 °C in the estimated temperature and 25–80 km in the estimated lithospheric thickness (Artemieva and Mooney, 2001).

High-resolution seismic velocity models have also been commonly used in defining the lithosphere. The crust and the high-velocity lid of the upper mantle above the seismic low velocity zone (LVZ) is often taken as the seismic lithosphere. The interface between the ‘lid’ and the LVZ, however, is far from being a distinct discontinuity, so the estimate of seismic lithosphere thickness ( $T_s$ ) is often subjected to ambiguity due to arbitrary definitions of the boundary between the ‘lid’ and the LVZ (Frederiksen et al., 2001; van der Lee, 2002; Feng et al., 2004); Zhu et al. (2002), for example, used some fixed velocities in defining the lithospheric base in studying the Chinese continent. Because the boundary between the ‘lid’ and the LVZ is not a discontinuity, the different definitions of the ‘boundary’ can cause variations of several tens of kilometers in the estimated lithospheric thickness. Another important problem is whether the seismic lithosphere estimated from short-time scale seismic information is equivalent to the long-time scale geodynamical lithosphere.

In Table 1, the thicknesses of the lithosphere as defined by the above three different methods are compared. They show considerable divergence from each other, both in active region as Tibet, and in relatively stable regions as the Tarim and Sino-Korean cratons. This difference may partly arise from errors in the observations, but most likely from the significant differences in the lithosphere definitions. The effective elastic lithosphere thickness may include only a part of the continental lithosphere (Burov and Diament, 1995), and obviously deviates from the thicknesses estimated from other definitions, therefore, we will no more discuss it. Since the physical properties of upper mantle are strongly affected by temperature (Pollack and Chapman, 1977), and temperature and its variation have direct geodynamic significance, the thermal definition of the lithospheric thickness  $T_t$  may be more reasonable to represent the thickness of a long-time scale lithosphere. However, as noted above, the estimate of  $T_t$  has notable uncertainties.

Recently, Goes et al. (2000) developed a method to estimate the upper mantle temperature by inverting seismic velocities using laboratory measurements of density and elastic moduli for various mantle minerals at high temperatures and pressures. By this method, it is no longer necessary to make the steady-state assumption or to use uncertain thermal parameters, but to directly estimate the 3D upper-mantle temperature structure from seismic velocities. This temperature estimation method has already been successfully applied in the studies of several continents (Goes et al., 2000; Röhm et al., 2000; Goes and Van der Lee, 2002; Cammarano et al., 2003; Shapiro and Ritzwoller, 2004). Using the upper-mantle temperatures estimated from high-resolution 3D seismic model, we can determine the lithospheric thickness, called seismic-thermal lithospheric thickness ( $T_{s-t}$ ), by using the definition that the lithosphere base coincides with the 1300 °C adiabat, as in the definition of the steady-state thermal lithosphere. In this paper, we first calculate the 3D upper-mantle temperature structure of the Chinese continent from the existing 3D seismic velocities; then estimate the lithospheric thickness from the calculated temperature.

## 2. Seismic model

Since LVZ S-velocity changes are more pronounced than changes in P-velocity and there is no P-velocity model with a resolution compatible with regional S-velocity model in the uppermost mantle beneath the Chinese continent, we only use an S-velocity model in this study. An S-velocity model for the upper mantle beneath the Chinese continent and its adjacent regions, referred as CN03S, is recently published by Huang et al. (2003). This model was resulted from fundamental-mode Rayleigh wave dispersion tomography study which used more than 4000 ray paths, and has a lateral resolution of 4–6° between 20°N and 45°N, i.e., west of Japan and the Ryukyu Islands, and east of Pamir and the Himalayas (Huang et al., 2003). Compared with other surface wave studies, Huang et al. (2003) used more records from small events at short epicentral distances to improve lateral resolution in the shallow depths. Local crustal thickness and tectonic information were used in the vertical S-velocity inversion by Herrmann’s program (Herrmann, 1987) from regionalized dispersions. However, since uncertainty estimation of the regionalized dispersions is too complex, no vertical resolution was given.

Using observation of Rayleigh wave group and phase velocities in 10–70 s period, an inversion (Rapine et al., 2003) by Herrmann’s program has a  $V_s$  uncertainty

of 0.02–0.1 km/s down to 120 km deep and a Moho depth uncertainty of  $\sim 10$  km at  $\sim 70$  km deep. An and Assumpção (in press) show a result (Snoko and James, 1997) from Rayleigh and Love phase and group velocities by Herrmann's program has a S-velocity difference of  $< \sim 0.04$  km/s in the upper mantle and a Moho depth difference of  $< 8$  km than by improved Genetic Algorithm (An and Assumpção, in press) and Neighbourhood Algorithm (Snoko and Sambridge, 2002). An inversion with Rayleigh wave group velocity would get worse resolution than with group and phase velocities (Shapiro and Ritzwoller, 2002). Here, we assume a  $V_s$  uncertainty of  $< 0.1$  km/s and the discontinuity depth uncertainty of  $\sim 30$  km in the uppermost mantle in CN03S. S-velocities in CN03S at a depth of 250 km are laterally very similar beneath the whole studied regions, implying that the model has bad resolution at depths  $\geq 250$  km. Thus, we only use the S-velocities in CN03S down to a depth of 240 km.

The velocity–temperature conversion used in this paper below is based on thermoelastic parameters estimated from isotropic aggregates. However, the model CN03S which was determined from Rayleigh waves gives vertical S-velocity information. Since the upper mantle may be radially anisotropic with different horizontal and vertical S-velocities (2–4% different; Dziewonski and Anderson, 1981), horizontal S-velocity information should be considered in addition to using vertical S-velocities for a study using isotropic aggregates. But Love waves observed in transverse component of a seismogram have more uncertainties/errors than Rayleigh waves in vertical component, so the horizontal S-velocities from a Love wave tomography will have more uncertainty than the vertical S-velocities from a Rayleigh wave study. So, there are fewer studies on Love waves than on Rayleigh waves. For these reasons, we did not use horizontal S-velocity information but only used the vertical S-velocities from Rayleigh waves.

### 3. Inversion for temperature from velocity

Based on laboratory measured thermoelastic properties of mantle minerals and models of the average mineralogical composition of the mantle, seismic velocities can be calculated for given temperature, pressure, composition, etc. We calculate S-velocity using the forward equations of Shapiro and Ritzwoller (2004) (see erratum at <http://ciei.colorado.edu/~nshapiro/PUBS/>), which is a slightly modified version from Goes et al. (2000). The elastic and anelastic constants and density and their dependence on temperature, pressure, and com-

position are taken from the mineral physics literatures, as in Goes et al. (2000).

The forward procedure to calculate seismic velocities takes into account both the anharmonic and the anelastic effects (Goes et al., 2000). Based on an infinitesimal strain approximation, the anharmonic part of the seismic velocities is calculated for given temperature, pressure, iron content, and mineralogical composition. The anelasticity parameters used in this study are from model  $Q_1$  in Goes et al. (2000), which is after Sobolev et al. (1996).

Forward calculation showed that temperature is the major parameter affecting seismic velocities in the depth range of 50–250 km (Jordan, 1979; Nolet and Zielhuis, 1994; Sobolev et al., 1996; Goes et al., 2000). The prominent compositional heterogeneity for different tectonic and geological provinces within continents is mainly caused by difference between the depleted or-cratonic mantle and the off-cratonic mantle (Shapiro and Ritzwoller, 2004). Sensitivity analysis (Goes et al., 2000) showed that the variations in velocity caused by the variations in upper mantle composition are relatively small, as compared with that caused by the variation in temperature, and are often below the level resolvable in seismic tomography. Therefore, seismic velocities have been used to directly invert for mantle temperatures (Goes and Van der Lee, 2002). Since most regions in the Chinese continent have a smaller tectonothermal age than a stable Precambrian craton, here we use the off-cratonic upper-mantle composition (Olivine 68%, Orthopyroxene 18%, Clinopyroxene 11%, Garnet 3%, and iron content 0.1; from Shapiro and Ritzwoller (2004)), and invert S-velocity for temperature with direct grid search.

Forward calculations (Goes et al., 2000) based on the experimental anharmonic and anelastic parameters showed that the uncertainties in the calculated upper-mantle temperature are  $\sim 150$  °C. Our tests show on-cratonic composition (Olivine 83%, Orthopyroxene 15%, Garnet 2%, and iron content 0.086; from Shapiro and Ritzwoller, 2004) can increase the estimated temperature by 15–120 °C compared to those made using the off-cratonic composition; more strongly temperature dependent anelasticity model  $Q_2$  (Goes et al., 2000) can lower a temperature estimates by 0–180 °C compared with estimates using model  $Q_1$ ; an S-velocity variation of 0.1 km/s can cause 50–250 °C temperature variation. We assume the same temperature uncertainty of 150 °C in this work as Goes et al. (2000).

The presence of melt and fluids (e.g., water) lowers the seismic velocities (Goes et al., 2000). Unfortunately, There is no model showing distribution of melt and fluids in the upper mantle beneath the Chinese continent,

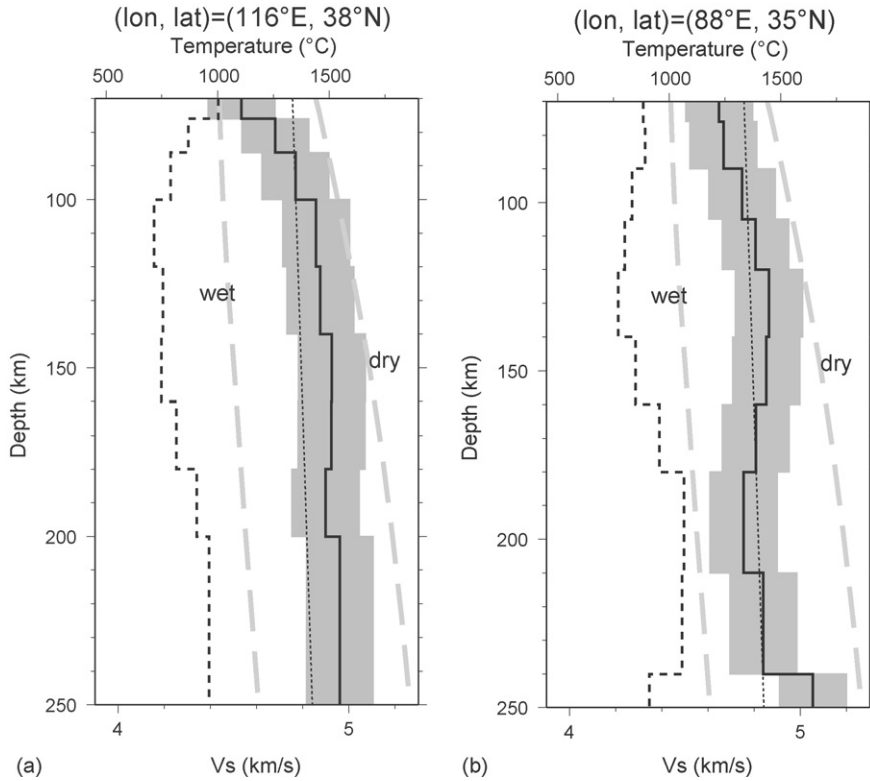


Fig. 2. Two S-velocity and seismic-thermal temperature 1D profiles. Black dashed line represents S-velocities from CN03S; solid line is seismic-thermal temperature profile with  $\pm 150^\circ\text{C}$  uncertainties (gray area); gray thick dashes are the wet and dry mantle solidi (Thompson, 1992); dotted line is the  $1300^\circ\text{C}$  adiabat.

therefore, we did not consider their effects in the conversion from velocity to temperature. If fluid-affected velocities are interpreted in terms of temperatures, the estimated temperatures would be too high. Thus the estimated mantle temperature in this paper should be taken as the upper bound.

#### 4. Results and interpretation

Since the deepest Moho of the Chinese continent is at the depth of  $\sim 70$  km under the Tibet and the seismic model of CN03S has good resolution down to the depth of  $\sim 240$  km, we only invert for the upper-mantle temperatures in the depth of 70–240 km. Fig. 2 shows two examples of 1D velocity and converted temperature profiles. Using a surface temperature of  $10^\circ\text{C}$  and the converted seismic-thermal temperatures at 80 km deep as boundary conditions and other thermal parameters from Wang (2001) and others, we calculated steady-state conductive thermal structure down to 80 km. The calculated surface heat flow (An and Shi, 2006) in most regions with dense heat flow observations has a misfit (Fig. 3) within an uncertainty range of  $-20\%$  to  $20\%$  which is the uncer-

tainty range for observations of highest and medium quality (Powell et al., 1988). So our calculated seismic-thermal temperatures at the depth of 80 km are consistent with the surface heat flow observations. All 3D crustal and upper-mantle temperature models are discussed in detail in another paper (An and Shi, 2006). Defining the lithospheric base to coincide with the topmost position with a temperature crossing the  $1300^\circ\text{C}$  adiabat (Jaupart and Mareschal, 1999; Artemieva and Mooney, 2001), we estimate the seismic-thermal lithosphere thicknesses ( $T_{s-t}$ ) of the Chinese continent (see Figs. 4 and 5). The adiabatic temperatures are calculated using a mantle adiabatic gradient of  $0.5^\circ\text{C}/\text{km}$ , as done by Lee et al. (2001). In Fig. 2a, the temperature downwards increases and first crosses the  $1300^\circ\text{C}$  adiabat at the depth range of 85–100 km, which is taken as the lithospheric base. Near this depth range, the upper temperature bound (Fig. 2a) is higher than the dry mantle solidus. In Fig. 2b, the lithospheric base, the topmost position with a temperature crossing the  $1300^\circ\text{C}$  adiabat, is at the depth range of 105–120 km, and the upper temperature bound near this depth range is quasi-equal to the dry mantle solidus.

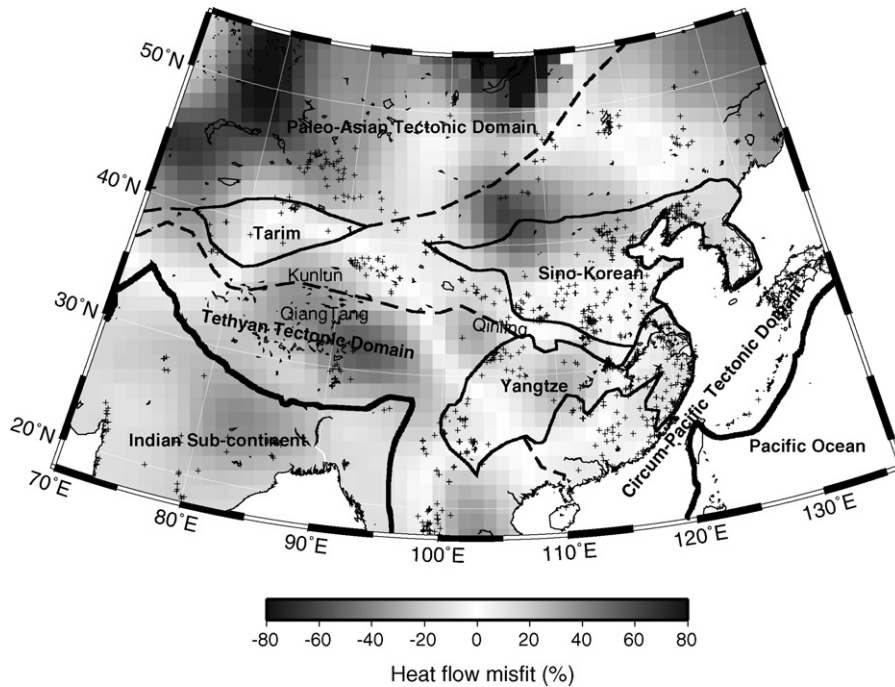


Fig. 3. Map of misfit ((obs. – pred.)/obs.) between observed and predicted surface heat flow. Crosses indicate heat flow observation positions.

Fig. 5 shows eastern China, including the Sino-Korean craton, eastern Yangtze craton, and southeast and northeast China, has a lithospheric thickness of  $\sim 100$  km. These regions have been strongly influenced by the tectonics of the circum-Pacific system (Ren et al., 1999). Central and western China, on the other hand, show thickened lithospheric belts subparallel to the collision zone between the Indian and Chinese continents. The south belt, the Tethyan tectonic domain including the Qinghai–Tibet plateau and the southwest to the Tarim craton, has a lithospheric thickness of  $\sim 160$ – $220$  km and may mark the cold subduction lithosphere of the Indian plate. The Kunlun–Qinling orogen and the neighbouring regions, along the north boundary of the Tethyan tectonic domain, have a lithospheric thickness of  $\sim 120$ – $150$  km.

A global Precambrian steady-state thermal lithosphere study (Artemieva and Mooney, 2001) showed correlation between crustal ages and lithospheric thicknesses, however, the age correlation is more complex at a regional scale (Simons and van der Hilst, 2002). The estimated seismic-thermal lithosphere thicknesses in Fig. 5 shows obvious dependence on the tectonic setting, such as the thick lithosphere of the Tethyan tectonic domain and the thinner lithosphere beneath eastern China (the circum-Pacific tectonic domain). The lithospheric thicknesses of the three cratons, ranging from  $\sim 170$  km beneath the Sichuan basin (the western

Yangtze craton),  $\sim 140$  km beneath the core of the Tarim craton,  $\sim 100$  km beneath the Sino-Korean craton (e.g., in Fig. 2a), and  $\sim 130$  km beneath the Ordos basin (the western Sino-Korean craton), are thinner than that of the young Tethyan tectonic domain, but the latter may include the subduction slab. Furthermore, the three cratons are also thinner than some cratons in other continents. For example, the North American Provinces ( $>1$  Ga) including the Slave craton has a seismic lithospheric thickness of  $\sim 250$  km (van der Lee, 2001); the Siberian platform (Priestley and Debayle, 2003) and Archean part of the Australian continent (Simons and van der Hilst, 2002) have a thickness of  $\sim 200$ – $250$  km. Thermal studies (Artemieva and Mooney, 2001 and references therein) showed that the Chinese Precambrian blocks are thin ( $\sim 100$ – $200$  km thick) too. The thin lithosphere of the Chinese cratons can be explained by that they have been reshaped by Phanerozoic tectonic activities (Ren et al., 1999) and then have a small tectonothermal age.

Fig. 4 shows four profiles across the major tectonic provinces in the Chinese continent. It shows that the top of the seismic LVZ corresponds closely with the  $1300^\circ\text{C}$  adiabat (solid lines in Fig. 4) in most regions. This correspondence, also found in Fig. 2, shows the physical correlation between the seismic low velocity and the average potential temperature of the convecting

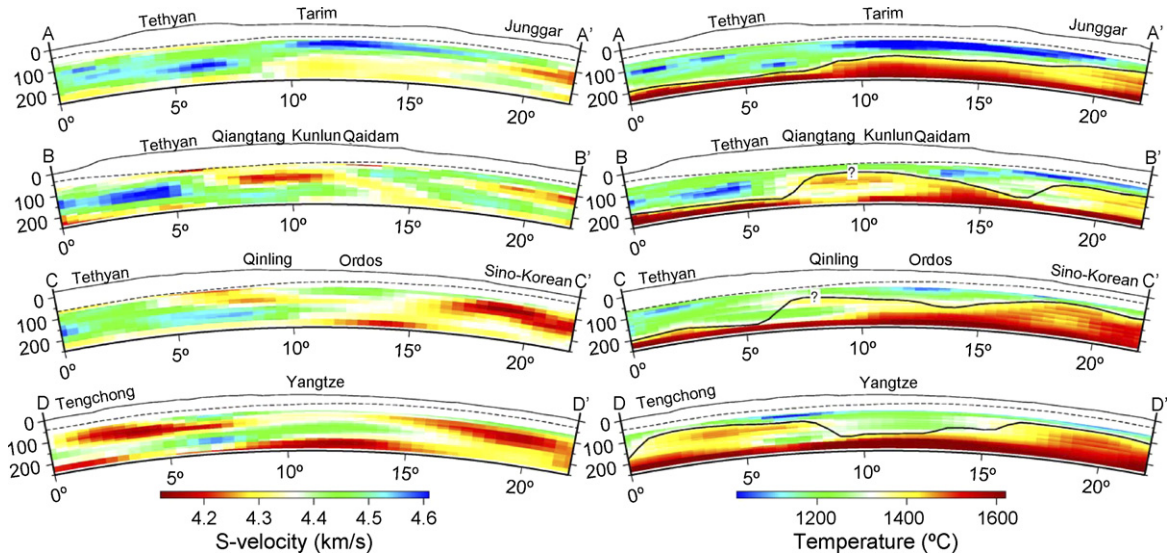


Fig. 4. 2D profiles of S-velocity (left column) and inverted temperature (right column) along the four transects marked in Fig. 5. Thin lines represent exaggerated topography. Dashes represent the Moho of the CRUST2.0 model (Bassin et al., 2000). Thick solid lines represent the 1300 °C adiabat, i.e., the base of the seismic-thermal lithosphere. Question marks (?) indicate locations where the lithosphere may be thicker than estimated (see text for discussion).

mantle, and implies that seismic lithosphere estimated from short-time scale seismic information may be equivalent to the long-time scale thermal lithosphere.

#### 4.1. Comparison between the estimated $T_{s-t}$ and $T_t$

Our seismic-thermal thicknesses (Fig. 5, profiles CC' and DD' in Fig. 4) under the Yangtze craton (~100–180 km) and the western Sino-Korean craton (the Ordos basin) (~130 km) are very similar to their corresponding thermal lithospheric thicknesses (Table 1). Since the seismic-thermal temperatures estimated from seismic velocities is related to the contemporary upper-mantle thermal state, and the steady-state temperature shows the ancient upper-mantle thermal state, their similarity implies a relatively long period of tectonic stability of the lithospheres under these two regions.

Under the Tarim craton, however,  $T_t$  (~250 km; Table 1) is much greater than  $T_{s-t}$  (~140–170 km; Fig. 5, profile AA' in Fig. 4), i.e., the seismic-thermal temperatures reach the 1300 °C adiabat at a much shallower depth than that calculated from surface thermal measurements and steady-state assumption. So the present-day seismic-thermal temperature at the base of the lithosphere under the Tarim craton is much higher than the temperature estimated by the steady-state thermal conduction. A reasonable explanation is that the high temperature in the lithosphere may be due to a recent tectonic event and that the heat from this high-temperature event has not yet reached the surface by thermal conduction.

The lithosphere of the Tibet (median massifs) has been shaped not only by the Cretaceous subduction of the cold oceanic Neo-Tethys lithosphere, but also by the collision with the Indian subcontinent and by the subduction of the cold Indian lid since Tertiary (Tapponnier et al., 2001). The cold upper mantle under Tibet, as shown by comparing the seismic-thermal lithosphere thickness (>~200 km; Fig. 5) with the steady-state thermal lithosphere thickness (<175 km; Table 1), may be a direct result of these tectonic activities besides the unreliability in steady-state thermal calculation with only few heat-flow observations (Hu et al., 2000) in the Tibet.

#### 4.2. Comparison between $T_{s-t}$ and $T_s$

Since the interface between the seismic lid and the LVZ is a gradual transition instead of a seismic discontinuity, there may be uncertainties in estimating the seismic lithosphere thicknesses, depending on the clarity of the LVZ and the steepness of the variation of seismic velocities with depth. If the seismic velocities decrease rapidly from lid to LVZ, the estimated seismic lithosphere thickness will have less uncertainty; otherwise, the uncertainties can be large. The conversion from seismic velocity to temperature represents a different way of looking at seismic information. It gives a physical explanation for seismic thickness, and certain features may show up more clearly because gradients look different. The profile AA' of Fig. 4 shows the S-velocity in low velocity zone under the Tarim craton has less variation,

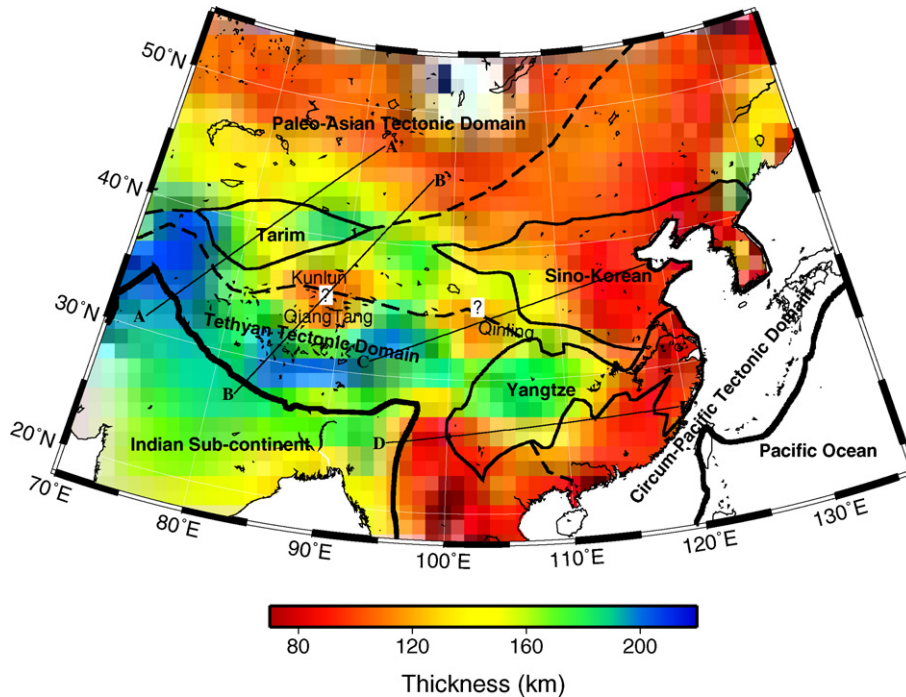


Fig. 5. Map of the estimated seismic-thermal lithospheric thicknesses of the Chinese continent. Also marked are the locations of four transects in Fig. 4. Question marks (?) indicate locations where the lithosphere may be thicker than estimated (see text for discussion).

however, the respective temperature obviously increases with depth down to 240 km deep.

#### 4.3. Lithospheric thickness ambiguity

The CN03S model showed a low-velocity belt (Huang et al., 2003) below the Moho extending eastward along the northern boundary of the Tethyan tectonic domain (see Fig. 5), i.e., nearly along the (east) Kunlun and Qiangtang orogen. In a waveform study, Rodgers and Schwartz (1998) attributed the low-velocity anomaly under the Qiangtang terrane to either partial melting or rheologically weak back-arc mantle displaced related to the Tethyan oceanic subduction beneath the Lhasa terrane before the Indo-Eurasia continental collision. Our result (profile BB' in Fig. 4 and Fig. 2b) shows that the temperature at the location of low-velocity anomaly is higher than 1300 °C adiabat, e.g., at the depth of ~110–160 km (Fig. 2b) under the Qiangtang terrane.

At the depth of ~130 km under the Qiangtang terrane (profile BB' of Fig. 4), the velocity is ~0.15 km/s (~4%) lower (correspondingly, the temperature is ~100 °C (or ~10%) higher) than that in the neighbouring regions. The variation of mantle composition can only cause ~1% velocity variation (Goes et al., 2000). Therefore,

the compositional effect is not enough to cause this velocity difference (4%), and then fluid (partial melt or water) effects have to be considered. Some other regions in the low velocity belt show similar high temperatures, which may also imply melt or fluid effects in the upper mantle. The high-temperature anomaly mostly appeared in regions, which have experienced complex tectonic evolution and/or are influenced by strong tectonic activities.

Below ~150 km deep for the low-velocity belt beneath the Qiangtang terrane in Fig. 2b and profile BB' of Fig. 4, the high temperature decreases with depth, and then the high-temperature anomaly disappeared. The part below ~160 km deep in Fig. 2b has a lower temperature and should belong to lithosphere too, and then lithospheric base may be much deeper than the estimation in Fig. 5. Below ~200 km deep, the temperature beneath the Qiangtang terrane increases and then crosses the 1300 °C adiabat again at the depth of ~210 km (Fig. 2b and BB' in Fig. 4), which is similar to the depth (~160–220 km) of the 1300 °C adiabat beneath the Tibet. The temperature profiles CC' and BB' in Fig. 4 shows that the cold Indian subcontinent subduction slab at ~200 km deep continues to extend north beneath the Qiangtang terrane and Kunlun–Qinling orogen. If the lithospheric base is at the depth of ~200 km, the

Qiangtang terrane and Kunlun–Qinling orogen should have a thick (~200 km) lithosphere as the general Tethyan tectonic domain, however, the subduction slab is separated by a high temperature belt (~110–160 km deep in Fig. 2b) with the general Chinese continent.

## 5. Conclusion

The effective elastic lithosphere may be only a part of the continental lithosphere (Burov and Diament, 1995), and its thickness obviously deviates from the thicknesses estimated from other definitions. Since the physical properties of upper mantle are strongly affected by temperature, the definition of the thermal lithosphere should be more reasonable. However, the estimate of the steady-state thermal lithosphere thickness has obvious uncertainties. The seismic-thermal lithosphere thickness estimated on the basis of high-resolution seismic data and thermoelastic properties of minerals is thus more accurate than those based on other definitions.

The complex Phanerozoic tectonic activities determined the complex lithospheric structure and tectonics in the Chinese continent, which may be the cause for the different estimates of the lithospheric thickness in most regions based on the different definitions.

The 3D upper-mantle temperatures of the Chinese continent were obtained by using S-velocities. By comparing the seismic and temperature profiles, we found that the top of the seismic low velocity zone in upper mantle is in close correspondence with the position of first crossing the 1300 °C adiabat for most regions. This correspondence shows that the seismic low velocity zone may have physical relation with the average potential temperature of the convecting mantle, and seismic lithosphere estimated from short-time scale seismic information may be equivalent to the long-time scale geodynamical lithosphere.

The distribution of the lithospheric thickness in the Chinese continent is complex. Eastern China of the circum-Pacific tectonic domain, including northeast China, Sino-Korean craton, east Yangtze craton, and south China orogen, has a lithosphere with a thickness of ~100 km. The Tethyan tectonic domain, including the Qinghai–Tibet plateau and south to the Tarim craton, on the other hand, has a lithosphere of ~160–220 km thick, which may include part of the subduction slab of the Indian subcontinent. The lithospheric thicknesses of the three large para-platforms/cratons range from ~170 km for the western Yangtze, ~140 km for Tarim, ~100 km for Sino-Korean. The three cratons may have been reshaped by Phanerozoic tectonic activities and

are thinner than most cratons in other continents. The estimated thicknesses show good correlation with the tectonic setting.

## Acknowledgements

We are grateful to Prof. Zhong-Xian Huang to share his good S-velocity results and for his good comments. We would particularly thank S. Goes for her thoughtful and constructive comments and suggestions, and Prof. Chi-Yuen Wang for his valuable fine comments and suggestions. We thank N.M. Shapiro for his suggestions to help improve the temperature estimation. This work is supported by China Postdoctoral Science Foundation, partly by the National Natural Science Foundation of China (NSFC-40234042 and 40374038) and a renovation fund (KZCX3-SW-138) from the Chinese Academy of Sciences. All figures are generated using the Generic Mapping Tools (GMT) (Wessel and Smith, 1991).

## References

- An, M., Assumpção, M.S., in press. Crustal and upper mantle structure in intracratonic Paraná Basin, SE Brazil, from surface wave dispersion using genetic algorithm. *J. South Am. Earth Sci.*
- An, M., Shi, Y., 2006. 3D crustal and upper-mantle temperature of the Chinese continent. *Sci. Chin. (Ser. D)*, submitted for publication.
- Artemieva, I.M., Mooney, W.D., 2001. Thermal thickness and evolution of Precambrian lithosphere: a global study. *J. Geophys. Res.* 106 (B8), 16387–16414.
- Bassin, C., Laske, G., Masters, G., 2000. The current limits of resolution for surface wave tomography in North America. *EOS Trans. AGU* 81, F897.
- Braitenberg, C., Wang, Y., Fang, J., Hsu, H.T., 2003. Spatial variations of flexure parameters over the Tibet–Qinghai plateau. *Earth Planet. Sci. Lett.* 205, 211–224.
- Burov, E.B., Diament, M., 1995. The effective elastic thickness ( $T_e$ ) of continental lithosphere: what does it really mean? *J. Geophys. Res.* 100 (B3), 3905–3927.
- Cammarano, F., Goes, S., Vacher, P., Giardini, D., 2003. Inferring upper-mantle temperatures from seismic velocities. *Phys. Earth Planet. Int.* 138 (3/4), 197–222.
- Dziewonski, A.M., Anderson, D.L., 1981. Preliminary reference earth model. *Phys. Earth Planet. Int.* 25 (4), 297–356.
- Feng, M., Assumpção, M.S., van der Lee, S., 2004. Group-velocity tomography and lithospheric S-velocity structure of the South American continent. *Phys. Earth Planet. Int.* 147, 315–331.
- Frederiksen, A.W., Bostock, M.G., Cassidy, J.F., 2001. S-wave velocity structure of the Canadian upper mantle. *Phys. Earth Planet. Int.* 124, 175–191.
- Goes, S., Govers, R., Vacher, P., 2000. Shallow mantle temperatures under Europe from P and S wave tomography. *J. Geophys. Res.* 105 (B5), 11153–11169.
- Goes, S., Van der Lee, S., 2002. Thermal structure of the North American uppermost mantle inferred from seismic tomography. *J. Geophys. Res.* 107 (B3), 2050.
- Herrmann, R.B., 1987. *Computer Programs in Seismology*. St. Louis University, St. Louis, MO.

- Hu, S., He, L., Wang, J., 2000. Heat flow in the continental area of China: a new data set. *Earth Planet. Sci. Lett.* 179 (2), 407–419.
- Huang, Z., Su, W., Peng, Y., Zheng, Y., Li, H., 2003. Rayleigh wave tomography of China and adjacent regions. *J. Geophys. Res.* 108 (B2), 2073.
- Jaupart, C., Mareschal, J.C., 1999. The thermal structure and thickness of continental roots. *Lithos* 48, 93–114.
- Jin, Y., McNutt, M.K., Zhu, Y.S., 1996. Mapping the descent of Indian and Eurasian plates beneath the Tibetan plateau from gravity anomalies. *J. Geophys. Res.* 101 (B5), 11275–11290.
- Jordan, T.H., 1979. Mineralogies, densities and seismic velocities of garnet lherzolites and their geophysical implications. In: Boyd, F.R., Myer, H.O.A. (Eds.), *The Mantle Sample: Inclusions in Kimberlites and Other Volcanics*. AGU, Washington, DC, pp. 1–14.
- Lee, C.-T., Yin, Q., Rudnick, R.L., Jacobsen, S.B., 2001. Preservation of ancient and fertile lithospheric mantle beneath the southwestern United States. *Nature* 411, 69–73.
- Lyon-Caen, H., Molnar, P., 1983. Constraints on the structure of the Himalaya from an analysis of gravity anomalies and a flexural model of the lithosphere. *J. Geophys. Res.* 88, 8171–8192.
- Lyon-Caen, H., Molnar, P., 1984. Gravity anomalies and the structure of the western Tibet and the southern Tarim basin. *Geophys. Res. Lett.* 11, 1251–1254.
- Mareschal, J.C., Jaupart, C., 2004. Variations of surface heat flow and lithospheric thermal structure beneath the North American craton. *Earth Planet. Sci. Lett.* 223, 65–77.
- McNutt, M.K., Diament, M., Kogan, M.G., 1988. Variations of elastic thickness at continental thrust belts. *J. Geophys. Res.* 93, 8825–8838.
- Nolet, G., Zielhuis, A., 1994. Low S velocities under the Tornquist–Teisseyre zone: evidence for water injection into the transition zone by subduction. *J. Geophys. Res.* 99, 15813–15820.
- Pollack, H.N., Chapman, D.S., 1977. On the regional variation of heat flow, geotherms, and lithospheric thickness. *Tectonophysics* 38, 279–296.
- Powell, W.G., Chapman, D.S., Balling, N., Beck, A.E., 1988. Continental heat flow density. In: Haenel, R., Rybach, L., Stegens, L. (Eds.), *Handbook of Terrestrial Heat-Flow Density Determination*. Kluwer Academic Publishers, pp. 167–222.
- Priestley, K., Debayle, E., 2003. Seismic evidence for a moderately thick lithosphere beneath the Siberian Platform. *Geophys. Res. Lett.* 30 (3), 1118.
- Rapine, R., Tilmann, F., West, M., Ni, J., Rodgers, A., 2003. Crustal structure of northern and southern Tibet from surface wave dispersion analysis. *J. Geophys. Res.* 108 (B2), 2120.
- Ren, J., Wang, Z., Chen, B., Jiang, C., Niu, B., Li, J., Xie, G., He, Z., Liu, Z., 1999. *The Tectonics of China from a Global View—A Guide to the Tectonic Map of China and Adjacent Regions*. Geological Publishing House, Beijing, pp. 32.
- Rodgers, A.J., Schwartz, S.Y., 1998. Lithospheric structure of the Qiangtang terrane, northern Tibetan Plateau, from complete regional waveform modeling: evidence for partial melt. *J. Geophys. Res.* 103 (B4), 7137–7152.
- Röhm, A.H.E., Snieder, R., Goes, S., Trampert, J., 2000. Thermal structure of continental upper mantle inferred from S-wave velocity and surface heat flow. *Earth Planet. Sci. Lett.* 181, 395–407.
- Shapiro, N.M., Ritzwoller, M.H., 2002. Monte-Carlo inversion for a global shear-velocity model of the crust and upper mantle. *Geophys. J. Int.* 151, 88–105.
- Shapiro, N.M., Ritzwoller, M.H., 2004. Thermodynamic constraints on seismic inversions. *Geophys. J. Int.* 157, 1175–1188.
- Simons, F.J., van der Hilst, R.D., 2002. Age-dependent seismic thickness and mechanical strength of the Australian lithosphere. *Geophys. Res. Lett.* 29 (11), 1529.
- Snoke, J.A., James, D.E., 1997. Lithospheric structure of the Chaco and Paraná Basins of South America from surface-wave inversion. *J. Geophys. Res.* 102, 2939–2951.
- Snoke, J.A., Sambridge, M., 2002. Constraints on the S wave velocity structure in a continental shield from surface wave data: comparing linearized least squares inversion and the direct search neighbourhood algorithm. *J. Geophys. Res.* 107 (B5).
- Sobolev, S.V., Zeyen, H., Stoll, G., Werling, F., Altherr, R., Fuchs, K., 1996. Upper mantle temperatures from teleseismic tomography of French Massif Central including effects of composition, mineral reactions, anharmonicity, anelasticity and partial melt. *Earth Planet. Sci. Lett.* 139 (1/2), 147–163.
- Tapponnier, P., Xu, Z., Roger, F., Meyer, B., Arnaud, N., Wittlinger, G., Yang, J., 2001. Oblique stepwise rise and growth of the Tibet Plateau. *Science* 294 (5547), 1671–1677.
- Teng, J., 1994. The seismic study of lithospheric physics in China. *Acta Geophys. Sin.* 37 (Suppl. I), 140–159.
- Thompson, A.B., 1992. Water in the earth's upper mantle. *Nature* 358, 295–302.
- van der Lee, S., 2001. Deep below North America. *Science* 294 (5545), 1297–1298.
- van der Lee, S., 2002. High-resolution estimates of lithosphere thickness from Missouri to Massachusetts, USA. *Earth Planet. Sci. Lett.* 203, 15–23.
- Wang, J.Y., 1996. *Geothermics in China*. Seismological Press, Beijing, pp. 300.
- Wang, Y., 2001. Heat flow pattern and lateral variations of lithosphere strength in China mainland: constraints on active deformation. *Phys. Earth Planet. Int.* 126, 121–146.
- Wang, Y., Wang, J., Xiong, L., Deng, J., 2001. Lithospheric geothermics of major geotectonic units in China mainland. *Acta Geosci. Sin.* 22 (1), 17–22.
- Wang, Y., Xu, H., 1996. The variations of lithospheric flexural strength and isostatic compensation mechanisms beneath the continent of China and vicinity. *Chin. J. Geophys.* 39 (Suppl.), 105–113.
- Watts, A.B., Burov, E.B., 2003. Lithospheric strength and its relationship to the elastic and seismogenic layer thickness. *Earth Planet. Sci. Lett.* 213, 113–131.
- Wessel, P., Smith, W.H.F., 1991. Free software helps map and display data. *EOS Trans. AGU* 72, 411.
- Zhao, L., Jiang, X., Jin, Y., Jin, X., 2004. Effective elastic thickness of continental lithosphere in western China. *Earth Sci. -J. Chin. Univ. Geosci.* 29 (2), 183–190.
- Zhu, J., Cao, J., Cai, X., Yan, Z., Cao, X., 2002. High resolution surface wave tomography in East Asia and West Pacific marginal seas. *Chin. J. Geophys.* 45 (5), 679–698.